

Velocity trapping in the lifted TASEP and the true self-avoiding random walk

Brune Massoulié,¹ Clément Erignoux,² Cristina Toninelli,^{3,1} and Werner Krauth^{4,5,6}

¹*CEREMADE, CNRS, Université Paris-Dauphine, Université PSL, 75016 Paris, France*

²*Inria MUSICS, ICJ UMR5208, CNRS, Ecole Centrale de Lyon,*

INSA Lyon, Université Claude Bernard Lyon 1,

Université Jean Monnet, 69603 Villeurbanne, France

³*DMA, ENS Université PSL, 45 rue d'Ulm 75005 Paris, France*

⁴*Laboratoire de Physique de l'Ecole normale supérieure, ENS, Université PSL,*
CNRS, Sorbonne Université, Université de Paris Cité, Paris, France

⁵*Rudolf Peierls Centre for Theoretical Physics, Clarendon Laboratory, Oxford OX1 3PU, UK*

⁶*Simons Center for Computational Physical Chemistry,*
New York University, New York (NY), USA

(Dated: March 14, 2025)

We discuss non-reversible Markov-chain Monte Carlo algorithms that, for particle systems, rigorously sample the positional Boltzmann distribution and that have faster than physical dynamics. These algorithms all feature a non-thermal velocity distribution. They are exemplified by the lifted TASEP (totally asymmetric simple exclusion process), a one-dimensional lattice reduction of event-chain Monte Carlo. We analyze its dynamics in terms of a velocity trapping that arises from correlations between the local density and the particle velocities. This allows us to formulate a conjecture for its out-of-equilibrium mixing time scale, and to rationalize its equilibrium superdiffusive time scale. Both scales are faster than for the (unlifted) TASEP. They are further justified by our analysis of the lifted TASEP in terms of many-particle realizations of true self-avoiding random walks. We discuss velocity trapping beyond the case of one-dimensional lattice models and in more than one physical dimensions. Possible applications beyond physics are pointed out.

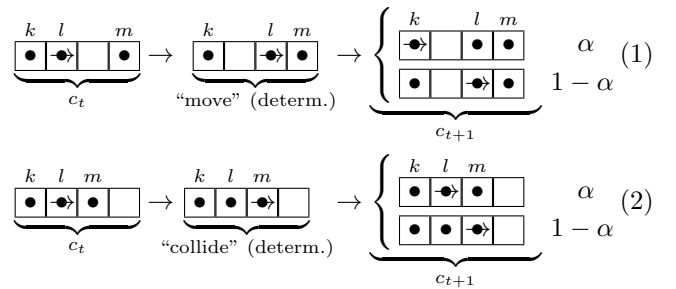
All of statistical mechanics descends from the insight that the equilibrium motion of atoms in a classical gas, liquid, or solid, etc., obeys the distribution obtained by Maxwell in 1859 [1]. For two phases of a material (say, a gas and a crystal) in thermal contact in a sample, atoms thus have the same instantaneous velocity distribution independent of (decoupled from) whether they weakly interact in the gas, or are tightly confined in the crystal lattice. The decoupling of the kinetic from the potential degrees of freedom underlies the microscopic interpretation of the temperature.

In computational physics, the decoupling of velocities and positions is ubiquitous. In the vast field of classical molecular dynamics [2–4], for example, the particle velocities in a finite system evolve with the gradient of the potential, but are furthermore updated from a thermostat, i.e., a Gaussian distribution specified by the system temperature. In Hamiltonian Monte Carlo [5, 6], a rigorous version of molecular dynamics, all particle velocities are periodically resampled from the Maxwell distribution in a way that is blind to its environment. The independence of positions and velocities is echoed in Monte Carlo methods [7] that at each time step attempt to move a random particle.

In recent years, non-reversible event-chain Monte Carlo methods [8–10] based on lifted Markov chains [11, 12] have featured faster convergence than possible under physical dynamics [13–15]. They exactly sample the Boltzmann distribution of the positions. Velocities, generalized into lifting variables, do not follow the Maxwell distribution, and they correlate with local

particle densities. In the present paper, we analyze the superdiffusive convergence of these algorithms. We justify the observed link [16, 17] between one-dimensional event-chain algorithms [18, 19] and true self-avoiding random walks (TSAW) [20], that were much studied in physics [21–23] and in mathematics [24–27].

For concreteness, we consider the lifted TASEP [28] (totally asymmetric simple exclusion process), a non-reversible Markov chain for N hard-sphere particles on a periodic one-dimensional L -site lattice. In the lifted TASEP, a single particle carries a pointer and can move, but the dynamics also determines which particle can move next:



Between times t and $t+1$, the active particle (here l) first moves to its right, keeping the pointer (eq. (1)) or, if this is not possible, first collides with its right-hand neighbor m , passing the pointer on to it (eq. (2)). Then, in both cases, with probability $\alpha > 0$, the pointer is pulled back from the active particle to its left-hand neighbor (from l to k or from m to l). With periodic boundary conditions, the above dynamics converges towards a sta-

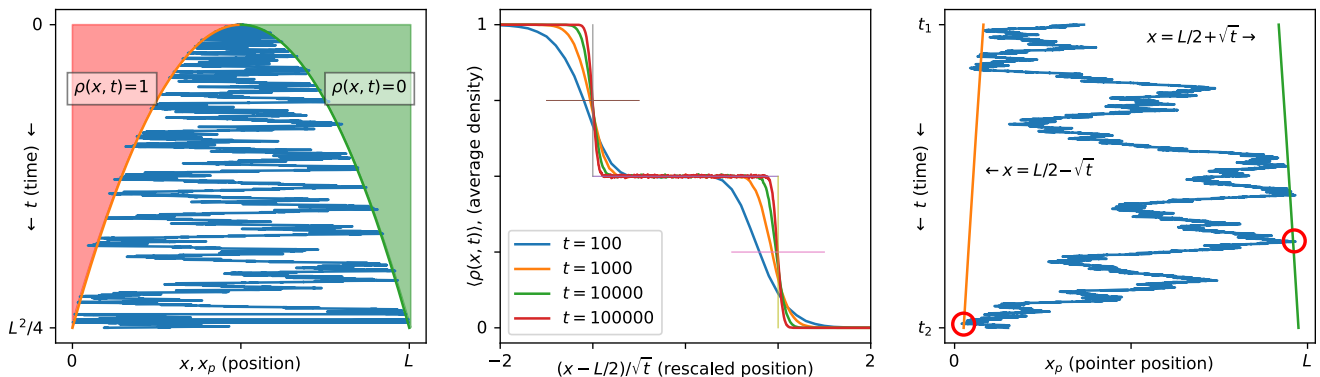


FIG. 1. Time evolution of the lifted TASEP ($N = 10^6, L = 2N$) at $\alpha = \alpha_{\text{crit}} = \frac{1}{2}$, from an initial “step” (at $t = 0, \rho(x < L/2) = 1$ and $\rho(x > L/2) = 0$). (a): Pointer position x_p vs time t , showing the dome-shaped critical region \mathcal{C}_t expanding at the expense of the step. (b): Ensemble-averaged density $\langle \rho(x, t) \rangle$, for rescaled positions $(x - L/2)/\sqrt{t}$ (the pointer position is excluded from the histogram of densities). The critical region appears clearly, and the ensemble-averaged interfaces have width $\sim t^{1/4}$. (c): Close-up of trajectory, between boundaries $L/2 \pm \sqrt{t}$ of the critical region. A pair of events defining a transfer is highlighted.

tionary state with, for any pullback α , equal weights for all lifted configurations c (positions of particles and of the pointer) [28].

In the lifted TASEP, only the active particle is responsible for mass transport which, in one time step, equals either one (as in eq. (1)) or zero (as in eq. (2)). The pullback α decouples the mass transport from the pointer drift v_{\rightarrow} , the difference between pointer positions in c_{t+1} and c_t (periodic boundary conditions being accounted for). Two averages of the pointer drift v_{\rightarrow} are relevant:

$$\underbrace{\langle v_{\rightarrow} \rangle}_{\text{equilibrium-averaged, } \bar{\rho} = N/L} = 1 - \frac{\alpha}{\bar{\rho}} \quad \text{and} \quad \underbrace{v_{\rightarrow}(\rho_{\ell}, \alpha)}_{\text{coarse-grained}} = \frac{\rho_{\ell} - \alpha}{\rho_{\ell}}. \quad (3)$$

On the left-hand side of eq. (3), the equilibrium-averaged pointer drift is expressed in terms of the system density $\bar{\rho} = N/L$, and it rigorously vanishes for $\alpha = \alpha_{\text{crit}} = \bar{\rho}$ [28]. The expression on the right-hand-side of eq. (3) translates this relation to the case of a pointer inside a local region of suitably chosen size ℓ with a coarse-grained local density ρ_{ℓ} . For the critical pullback α_{crit} , the pointer drift

$$v_{\rightarrow}(\rho_{\ell}, \alpha_{\text{crit}}) = \frac{\rho_{\ell} - \alpha_{\text{crit}}}{\rho_{\ell}} = \frac{\Delta\rho_{\ell}}{\rho_{\ell}} \quad (4)$$

exposes a linear coupling to the local excess density $\Delta\rho_{\ell} = \rho_{\ell} - \bar{\rho}$.

The pointer-drift–density coupling of eq. (4) contains the mechanism that traps the pointer. This is most notable when starting the lifted TASEP at α_{crit} from a “step” initial configuration at time $t = 0$ with the left-hand side of the system at high local density $\rho^{\text{high}} > \bar{\rho}$, and the right-hand side at low density $\rho^{\text{low}} < \bar{\rho}$ (see Fig. 1a). From an initial position x in the high-density region (where $v_{\rightarrow} > 0$) the pointer is expelled towards the right, and from a low-density region it is expelled to-

wards the left. Trapped in the middle, the pointer moves back and forth, creating a dome-shaped critical region \mathcal{C}_t , which expands while maintained in equilibrium at density $\sim \bar{\rho}$. The scaling behavior of the ensemble-averaged density $\rho(x, t)$ starting from the step initial configuration defines \mathcal{C}_t precisely as the region with an asymptotic density $\bar{\rho}$ (see Fig. 1b). Although the ensemble average represented in Fig. 1b spreads the position of the interface by $\sim t^{1/4}$ around its expected position, the critical region is bounded by sharp interfaces, which trap the pointer through the mechanism of eq. (3). Its size $|\mathcal{C}_t|$ for the step initial configuration with $\rho^{\text{high,low}} = (1, 0)$ (the case shown in Fig. 1) follows from assuming the pointer to be uniformly distributed in \mathcal{C}_t . Since a unit mass transport (eq. (1)) occurs with probability $\frac{1}{2}$, each point of the critical region moves forward by $\frac{1}{2|\mathcal{C}_t|}$ in one step, expanding it in both directions (because the leftmost particle pushes an empty site backwards):

$$|\mathcal{C}_{t+1}| \simeq |\mathcal{C}_t| + \frac{1}{|\mathcal{C}_t|}. \quad (5)$$

This difference equation for $|\mathcal{C}_t|$ (with $|\mathcal{C}_0| \sim 1$) is solved by $|\mathcal{C}_t| = 2\sqrt{t}$ for large t , an expression well confirmed for the single trajectory of Fig. 1a and for the ensemble average of trajectories of Fig. 1b.

The analysis of eq. (5) generalizes to a density step $\rho^{\text{high,low}} = \bar{\rho} \pm \varepsilon$, resulting in

$$|\mathcal{C}_t| = 2\sqrt{t/(2\varepsilon)} \quad (\rho^{\text{high,low}} = \bar{\rho} \pm \varepsilon). \quad (6)$$

This dimensionally corrected version of the solution to eq. (5) is backed up by numerical solutions analogous to Fig. 1b [29]. It incorporates that any excess particle, at density $\bar{\rho}$, must be spread out over a distance $\sim 1/\varepsilon$ if the initial density beyond the right boundary is $\bar{\rho} - \varepsilon$. In equilibrium, step-like initial configurations with $\varepsilon \sim L^{-1/2}$

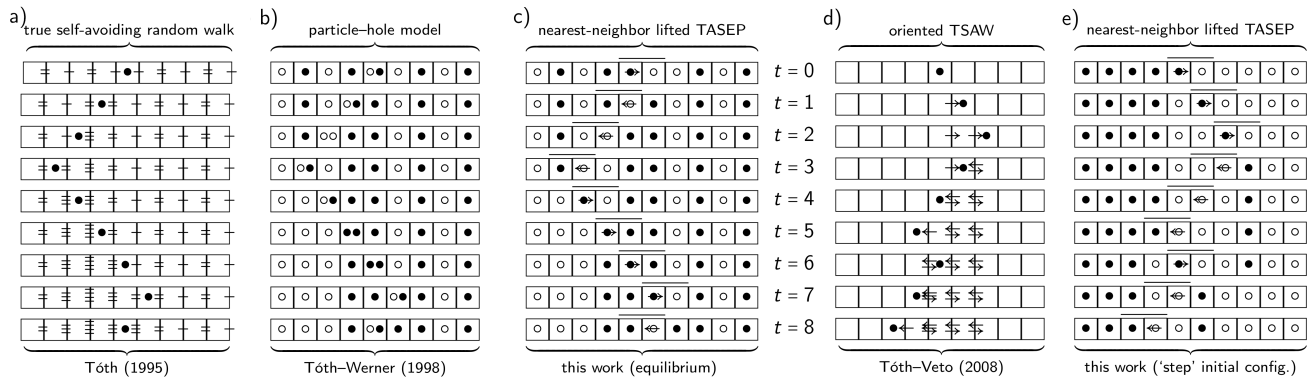


FIG. 2. Correspondence of TSAW’s with particle models related to the lifted TASEP. (a): Zero-temperature version of the TSAW introduced in Ref. [24], with local times indicated by horizontal lines, initialized as in Ref. [25]. (b): Particle-hole representation of (a) [25]. From the doubly occupied site, a particle moves to the right, or a hole to the left. (c): Equivalent representation of (a) in terms of the nearest-neighbor lifted TASEP of eqs. (8) to (10). (d): Oriented TSAW with directional local times as initialized in Ref. [26]. (e): Equivalent representaton of (d) in terms of the nearest-neighbor lifted TASEP, with a “step” initial configuration.

arise from thermal particle-number fluctuations. From eq. (6), the time scale on which such a step spreads to the system-size scale L is given by

$$t_{\text{eq}} \sim L^{3/2}. \quad (7)$$

The equilibrium fluctuations in the L -site lifted TASEP are thus expected to reset on a superdiffusive time scale $L^{3/2}$ that naturally arises from the length scale L together with the velocity scale $L^{-1/2}$ of eq. (4) for equilibrium density fluctuations. The time scale t_{eq} is a prime candidate for the relaxation time (the inverse absolute gap) of the lifted TASEP, and it is readily seen in numerical simulations [19, 28, 30]. However, numerical Bethe-ansatz solutions of the lifted TASEP transition matrix [28, 31] point to the existence of a (possibly isolated) eigenvalue with a spectral gap scaling as $1/L^2$ and suggesting that, strictly speaking, the relaxation time of the lifted TASEP (for $N \propto L$ and $\alpha = \alpha_{\text{crit}}$) may be $\sim L^2$. Up to this possible subtlety, we conjecture that in equilibrium not only the pointer travels through the system L in time $\sim L^{3/2}$ (and likewise, through the critical region in time $\sim |\mathcal{C}_t|^{3/2}$), but also that each of its passes through the lattice produces an essentially independent equilibrium configuration.

The microscopic mechanism for the expansion of the critical region relies on a subtle interplay of equilibrium particle-number fluctuations with the pointer drift. For a single trajectory starting from the step initial configuration we treat the case $\alpha = 1/2$, $\rho^{\text{high,low}} = (1, 0)$ (see Fig. 1c). At a given time $t \lesssim L^2/4$, the size of the critical region is $|\mathcal{C}_t| \sim \sqrt{t}$. Our simulations confirm that the pointer requires $\delta t \sim |\mathcal{C}_t|^{3/2}$ steps to move across the critical region, which is consistent with it being maintained in equilibrium, driving the pointer in either direction through the effect of thermal fluctuations. During

each crossing, mass transport advances the particles in \mathcal{C}_t by $\delta n \sim |\mathcal{C}_t|^{3/2}/|\mathcal{C}_t| = |\mathcal{C}_t|^{1/2}$, expanding the critical region by the same order. A positive density fluctuation, for example, drives the pointer away from the left boundary and towards the right. It induces mass transport, which ultimately spreads the critical region towards the low-density region by $\sim |\mathcal{C}_t|^{1/2}$, thus lowering the density and eventually reversing the sign of the density fluctuation in \mathcal{C}_t . This then drives the pointer back to the left, towards the high-density region. Through each visit of the pointer at the left boundary of \mathcal{C}_t , mass is pushed forward, spreading \mathcal{C}_t to the left. Eventually, \mathcal{C}_t grows to the left by $\sim |\mathcal{C}_t|^{1/2}$, which once again reverses the density fluctuations. In order for \mathcal{C}_t to grow macroscopically (of order $|\mathcal{C}_t|$), this back-and-forth motion takes place $\sim |\mathcal{C}_t|^{1/2}$ times. Each pointer crossing of the critical region requires a time $\sim |\mathcal{C}_t|^{3/2}$ and it ultimately reverses the fluctuation, thus resulting in a macroscopic growth time scale $|\mathcal{C}_t|^2$. This mechanism is consistent with our previous estimate $\delta t \sim |\mathcal{C}_t|^{3/2}$ and $\delta n \sim |\mathcal{C}_t|^{1/2}$, and it supports the picture of the critical region in effective equilibrium.

The lifted TASEP is closely related to several true self-avoiding random walk (TSAW) models (see Fig. 2a-e, the shorthand TSAW(a) refers to the model illustrated in Fig. 2a [24], etc.). Self-avoiding random walks were originally introduced [20] in order to differentiate self-avoiding lattice polymers (which are not proper random walks) from “true” random walks that remember the number of previous passages (called “local times”) on each site. Renormalization arguments [21] indicate that a one-dimensional TSAW explores a region of size $\sim t^{2/3}$ in a time t . A variant [24] of the original model records the number of passages across edges (rather than on sites), allowing for a rigorous analysis. At zero temperature, on a one-dimensional infinite lattice, this TSAW(a) has

a particle move to either side with equal probabilities if the two neighboring edges have the same local time, and otherwise moves across the edge with the smaller of the two local times. It was proved for this model that for positive temperature, during a time t , the particle explores a region of size $t^{2/3}$ [24]. Unlike the random walk of the pointer itself, the combined evolution of the pointer and the local times is a Markov chain. Clearly, at zero temperature, this Markov chain requires initial non-constant local times in order to avoid pathological behavior. In this setting, the $t^{2/3}$ scaling likely still holds, so that $t^{2/3} = L$ agrees with the $3/2$ exponent of eq. (7). In Ref. [25, Sect. 11], it is shown that TSAW(a) is equivalent to TSAW(b), namely a lattice model of particles and holes, where a single site contains a pair of items (either two particles, two holes, or a particle and a hole). In TSAW(b), at each time step, one of the two paired items, chosen randomly, moves to the left if it is a hole and to the right if it is a particle.

The models TSAW(a,b) are furthermore equivalent to the nearest-neighbor lifted TASEP (see Fig. 2c) [29], defined by the transitions

$$\begin{array}{|c|c|} \hline \bullet & \bullet \\ \hline \end{array} \rightarrow \begin{array}{|c|c|} \hline \bullet & \bullet \\ \hline \end{array} \quad p = 1 \quad (8)$$

$$\begin{array}{|c|c|} \hline \circ & \leftarrow \\ \hline \end{array} \rightarrow \begin{array}{|c|c|} \hline \leftarrow & \circ \\ \hline \end{array} \quad p = 1 \quad (9)$$

and

$$\left. \begin{array}{|c|c|} \hline \bullet & \circ \\ \hline \circ & \leftarrow \\ \hline \end{array} \right\} \rightarrow \left\{ \begin{array}{|c|c|} \hline \leftarrow & \bullet \\ \hline \circ & \bullet \\ \hline \end{array} \quad p = \alpha \right. \\ \left. \begin{array}{|c|c|} \hline \bullet & \leftarrow \\ \hline \end{array} \quad p = 1 - \alpha. \right. \quad (10)$$

The configurations of the nearest-neighbor lifted TASEP have the same trajectories as in the lifted TASEP with a time change. In the nearest-neighbor lifted TASEP, when the pointer encounters a cluster of particles, it crosses it deterministically by eq. (8), whereas in the lifted TASEP, by eq. (2), this cluster is ultimately crossed but in a typically longer random time. Conversely, in the lifted TASEP, after a pullback move of eq. (1), the pointer crosses instantly the empty zone behind it, while in the nearest-neighbor lifted TASEP, this move is broken down into deterministic local steps of eq. (9). We can thus justify [29] that the two models have overall the same equilibrium and out-of-equilibrium time scales. This establishes the equivalence of the lifted TASEP with the TSAW(a) on an infinite lattice. On a lattice of length L with periodic boundary conditions, the nearest-neighbor lifted TASEP converges for all α to the stationary state with equal weights for all configurations. Finally, we consider the zero-temperature “oriented” TSAW(d), in which each edge records directional local times [26]. In order to jump away from a site, the two outgoing local times are compared. Started from all-zero local times, TSAW(d) is also equivalent to the nearest-neighbor lifted TASEP with a step initial configuration [29]. For TSAW(d), the scaling $|\mathcal{C}_t| \simeq 2\sqrt{t}$

and the uniform position of the pointer inside \mathcal{C}_t are evidenced in Ref. [26], which further justifies eq. (5). The nearest-neighbor lifted TASEP thus connects the original TSAW(a,b) [24, 25] and its oriented variant TSAW(d) [26], the former being an equilibrium version of the latter. The two variants map onto two different regimes of the lifted TASEP, namely an equilibrium-like and a step setting. The $t^{2/3}$ scaling of the pointer motion at zero temperature is supported by its continuous limit derived in Ref. [29], which yields the equation of the true self-avoiding motion [25], for which the $2/3$ exponent is proven.

In conclusion, the self-trapping of velocities in non-reversible Markov chains, that we described here for the lifted TASEP at the critical pullback α_{crit} , originates in velocity–density correlation, and it generates exceptionally fast local dynamics, both out of equilibrium and in equilibrium. The phenomenon extends to generic one-dimensional particle models on the lattice [31] or, under event-chain Monte Carlo dynamics, to the continuum [19, 30]. It has also been demonstrated in higher-dimensional models [32]. The lifted TASEP departs from the logic of gradient-based simulation methods, for example in the discussed dome-shaped expansion of the critical region. Particles far outside the dome are strictly arrested—they never receive the pointer. In consequence, they do not add to the computational burden for equilibrating the system. Non-equilibrium and equilibrium scalings are thus faster than for the (unlifted) TASEP and for Hamiltonian Monte Carlo. Remarkably, the lifted-TASEP time evolution is totally unbiased, and Metropolis corrections and resamplings as in Hamiltonian Monte Carlo are not needed. We expect the principles at work in the lifted TASEP to be of more general use in optimization and molecular simulation, where gradient-based and stochastic gradient-based methods are widespread but likely not optimal.

We thank F. H. L. Essler, K. Hukushima, A. C. Maggs, S. Todo, and B. Tóth for helpful discussions. Research of W. K. was supported by a grant from the Simons Foundation (Grant 839534, MET). W. K. thanks the Isaac Newton Institute for Mathematical Sciences, Cambridge, for support and hospitality during the programme Monte Carlo sampling: beyond the diffusive regime, where work on this paper was undertaken. This work was supported by EPSRC grant EP/Z000580/1. This work was supported by PSL via the GP Statistical Physics and Mathematics.

-
- [1] S. G. Brush, *The Kind of Motion We Call Heat: A History of the Kinetic Theory of Gases in the 19th Century* (North-Holland Publishing Company, 1976).
 [2] T. Schlick, *Molecular Modeling and Simulation: An Interdisciplinary Guide* (Springer-Verlag, 2002).

- [3] D. Frenkel and B. Smit, *Understanding Molecular Simulation: From Algorithms to Applications*, Computational science series (Elsevier Science, 2001).
- [4] G. Ciccotti, C. Dellago, M. Ferrario, E. R. Hernández, and M. E. Tuckerman, *Eur. Phys. J. B* **95**, 3 (2022).
- [5] S. Duane, A. Kennedy, B. J. Pendleton, and D. Roweth, *Phys. Lett. B* **195**, 216 (1987).
- [6] R. M. Neal, in *Handbook of Markov Chain Monte Carlo*, edited by S. Brooks, A. Gelman, G. Jones, and X.-L. Meng (Chapman and Hall/CRC, 2011) pp. 113–162.
- [7] W. Krauth, *Statistical Mechanics: Algorithms and Computations* (Oxford University Press, 2006).
- [8] E. P. Bernard, W. Krauth, and D. B. Wilson, *Phys. Rev. E* **80**, 056704 (2009).
- [9] M. Michel, S. C. Kapfer, and W. Krauth, *J. Chem. Phys.* **140**, 054116 (2014).
- [10] W. Krauth, *Front. Phys.* **9**, 229 (2021).
- [11] P. Diaconis, S. Holmes, and R. M. Neal, *Ann. Appl. Probab.* **10**, 726 (2000).
- [12] F. Chen, L. Lovász, and I. Pak, Proceedings of the 17th Annual ACM Symposium on Theory of Computing, 275 (1999).
- [13] E. P. Bernard and W. Krauth, *Phys. Rev. Lett.* **107**, 155704 (2011).
- [14] T. A. Kampmann, D. Müller, L. P. Weise, C. F. Vorsmann, and J. Kierfeld, *Front. Phys.* **9**, 96 (2021).
- [15] M. Klement and M. Engel, *J. Chem. Phys.* **150**, 174108 (2019).
- [16] A. C. Maggs, *EPL* **147**, 21001 (2024).
- [17] A. C. Maggs, Event-chain Monte Carlo and the true self-avoiding walk (2024), arXiv:2410.08694.
- [18] S. C. Kapfer and W. Krauth, *Phys. Rev. Lett.* **119**, 240603 (2017).
- [19] Z. Lei, W. Krauth, and A. C. Maggs, *Phys. Rev. E* **99**, 10.1103/physreve.99.043301 (2019).
- [20] D. J. Amit, G. Parisi, and L. Peliti, *Phys. Rev. B* **27**, 1635 (1983).
- [21] L. Pietronero, *Phys. Rev. B* **27**, 5887 (1983).
- [22] J. Bernasconi and L. Pietronero, *Phys. Rev. B* **29**, 5196 (1984).
- [23] J. Brémont, O. Bénichou, and R. Voituriez, *Phys. Rev. Lett.* **133**, 10.1103/physrevlett.133.157101 (2024).
- [24] B. Toth, *The Annals of Probability* **23**, 1523 (1995), publisher: Institute of Mathematical Statistics.
- [25] B. Tóth and W. Werner, *Probab. Theory and Relat. Fields* **111**, 375–452 (1998).
- [26] B. Toth and B. Veto, *Electron. J. Probab.* **13**, 10.1214/ejp.v13-570 (2008).
- [27] L. Dumaz and B. Tóth, *Stoch. Process. Their Appl.* **123**, 1454–1471 (2013).
- [28] F. H. L. Essler and W. Krauth, *Phys. Rev. X* **14**, 041035 (2024).
- [29] C. Erignoux, W. Krauth, B. Massoulié, and C. Toninelli (2025), manuscript in preparation.
- [30] W. Krauth, Hamiltonian Monte Carlo vs. event-chain Monte Carlo: an appraisal of sampling strategies beyond the diffusive regime (2024), arXiv:2411.11690 [cond-mat.stat-mech].
- [31] F. H. L. Essler, J. Gipouloux, and W. Krauth, Lifted TASEP: long-time dynamics, generalizations, and continuum limit (2025), arXiv:2502.16549 [cond-mat.stat-mech].
- [32] A. C. Maggs and W. Krauth, *Phys. Rev. E* **105**, 015309 (2022).